Carbohydrate Research 375 (2013) 55–62

Contents lists available at SciVerse ScienceDirect

Carbohydrate Research

journal homepage: www.elsevier.com/locate/carres

N-linked glycolipids by Staudinger coupling of glycosylated alkyl diazides with fatty acids

Salih Mahdi Salman [a,b], Thorsten Heidelberg [a,*], Hairul Anuar Bin Tajuddin [a]

[a] Chemistry Department, Faculty of Science, University of Malaya, Lembah Pantai, 50603 Kuala Lumpur, Malaysia
[b] Chemistry Department, Faculty of Medicine, University of Diyala, Diyala Governorate, Iraq

ARTICLE INFO

Article history:
Received 8 January 2013
Received in revised form 6 March 2013
Accepted 23 March 2013
Available online 3 April 2013

Keywords:
Staudinger reaction
Diazide
Tetrahydropyrimidine
Amide-based bio-surfactants
Bi-antennary glycolipids

ABSTRACT

Aiming for new glycolipids with enhanced chemical stability and close structural similarity to natural cell membrane lipids for the development of a drug delivery system, we have synthesized double amide analogs of glyco-glycerolipids. The synthesis applied a Staudinger reaction based coupling of a 1,3-diazide with fatty acid chlorides. While the concept furnished the desired glucosides in reasonable yields, the corresponding lactosides formed a tetrahydropyrimidine based 1:1 coupling product instead. This unexpected coupling result likely originates from steric hindrance at the iminophosphorane intermediate and provides an interesting core structure for potentially bioactive surfactants. The assembly behavior of both glycolipid types was investigated by optical polarizing microscopy, DSC and surface tension studies.

1. Introduction

Glycolipids are natural components of most cell membranes. Unlike the predominant phospholipids, glycolipids are selectively expressed on the exterior surface of the cellular membrane,[1,2] thus suggesting that they play an active role in cellular recognition[3,4] or exchange processes.[5] Their non-ionic nature provides advantages with respect to formulation applications, as aggregates are less likely to be affected by environmental changes, like pH or ion concentrations. Based on these aspects, glycolipids are good candidates for a vesicular delivery system of pharmaceutically active components.

All major amphiphilic components of the cell membrane are characterized by a bi-antennary lipid structure comprising a single hydrophilic head group and two hydrophobic alkyl chains, which commonly are derived from fatty acids. A typical glycolipid structure involves a glycerol spacer linking two fatty acids to the carbohydrate;[6–8] example structure **1,** as shown in Figure 1, utilizes a lactose head group, as oligosaccharides with this core structure are frequently found in nature[9] and lactose is the most economic reducing disaccharide. Unlike the glycosidic linkage between the glycerol and the sugar, the ester bonds between the polyol and the fatty acids are easily affected by hydrolysis under both acid and basic conditions. This sensitivity renders natural glycolipids non-favorable for delivery applications.

Several modifications have been suggested to increase the chemical stability of bi-antennary glycolipids. Examples involve replacement of the ester linkage by ethers,[10] as shown in structure **2**, or replacement of the entire diacyl glycerol by a branched chain alcohol,[11] see structure **3**. In both approaches the branching domain rather attributes to the hydrophobic region than to the hydrophilic, as in glycol-glycerolipids like **1**. This difference is not expected to alter the generic assembly behavior of lipids, which can be understood based on packing theory considerations.[12,13] However, it may affect the water profile around a delivery vesicle and, thus, have implications on the fusion of the vesicle with a cell membrane. In the desire to optimize the glycolipid structure for a vesicular delivery system, we, therefore, aimed for a branching core combining hydrophilic behavior with good chemical stability. Replacement of ester linkages with amide analogs appears to be a suitable concept. With respect to stereochemical implications, which complicate the synthesis and increase related costs, the 1-glycosylated glycerol core in **1** was changed into the symmetric 2-glycosylated analog, **2**,[10] as previously reported for both ester and ether based surfactants. This leads to target structure **4**.

2. Results and discussion

2.1. Synthesis

The synthetic concept was developed on glucose, prior to application to the more interesting lactose core. The sequence, displayed in Figure 2, involved glycosylation of commercially available

* Corresponding author. Tel.: +60 3 7967 7170; fax: +60 3 7967 4193.
E-mail address: heidelberg@um.edu.my (T. Heidelberg).

0008-6215/$ - see front matter © 2013 Elsevier Ltd. All rights reserved.
http://dx.doi.org/10.1016/j.carres.2013.03.028

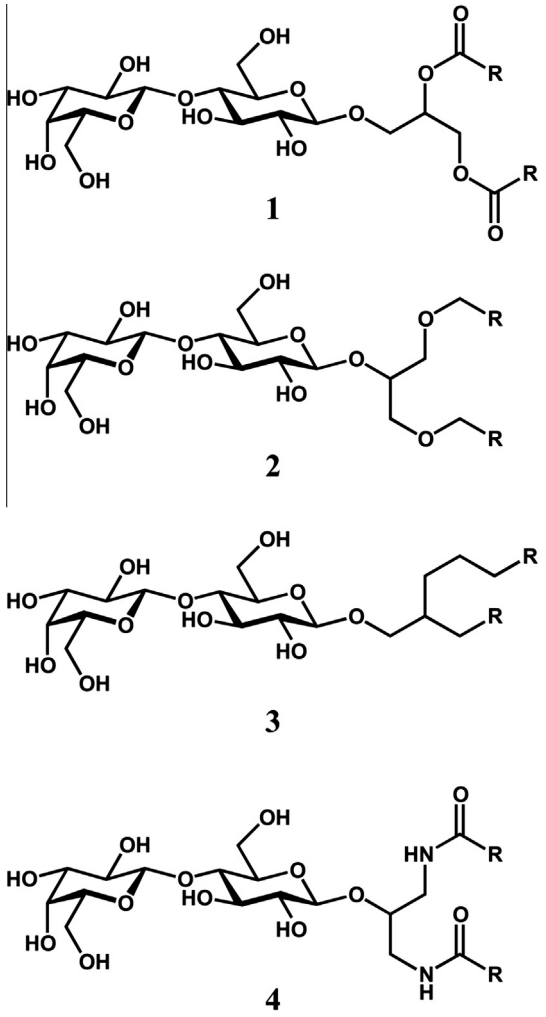

Figure 1. Structure comparison of natural and synthetic bi-antennary glycolipids.

1,3-dichloro-2-propanol followed by a subsequent substitution of the halide **6**[14] to obtain diazide **7**.[14] Economic considerations favor a Lewis acid catalyzed glycosylation based on peracetate **5**,[15] which selectively provides the desired β-anomer **6**, if boron trifluoride is applied in a short reaction time. The purification does not require chromatography, because both intermediate **6** and **7** can be crystallized.

The Staudinger based coupling[16,17] of fatty acid chlorides, varying in chain length from C_8 to C_{12}, with diazide **7** provided the expected diamides **8** in yields above 60%. Unlike in previous steps, chromatographic purification could not be avoided. Final deprotection under Zemplen conditions[18] furnished the glucoside surfactants **9a–c** in overall yields of 22–23% based on β-glucose pentaacetate.

Application of the synthetic approach to lactose, as shown in Figure 3, provided diazide **12**[19] in 48% yield based on lactose octaacetate **10**. Staudinger reactions with various fatty acid chlorides ranging from C_8 to C_{12}, however, failed to provide the expected diamide **13**. Instead the cyclic coupling products **14** were obtained in reproducible yields of 70%, which provided the corresponding surfactants **15a–c** upon deacetylation. Although phosphine mediated cyclizations of azido-amides have been reported previously,[20–22] the reaction product is rather unexpected. This does not only refer to the formation of tetrahydopyrimidines, which so far have been accessed by different strategies,[23–25] but particularly relates to the different behavior of glucose and lactose, despite identical stereochemistry at the reducing sugar.

In an attempt to explain the different behavior of the glucose and the lactose diazides **7** and **12** in Staudinger reactions, a molecular modeling study was performed. Structure optimization for the bis-iminophosphorane intermediate **16**, see Figure 4, led to the conformation depicted in Figure 5.† While the nitrogen atom of one of the two iminophosphoranes is easily accessible for reaction with the fatty acid chloride, the corresponding second reaction center is blocked by the non-reducing sugar of the lactose. This steric hindrance appears to be sufficient to block the intermolecular reaction, thus promoting the competing cyclization based on coupling of the remaining iminophosphorane with the initially formed first amide. The glucose-based bis-iminophosphorane, on the other hand, does not exhibit steric hindrance. For this, the higher reactivity of the fatty acid chloride explains the formation of the diamide surfactant type **8** instead of a tetrahydropyrimidine like in **14**.

The non-symmetric structure of the tetrahydro-pyrimidine ring gives rise to diastereomers. This is reflected in the NMR spectra of compounds **14** and **15**, which indicate two products. Table 1 does not reveal any trend for a correlation of chain length with diastereomeric ratio. This suggests that minor variations of the reaction parameters may have significant effects.

2.2. Physical properties

All surfactants of type **9** only exhibited a crystalline or gel solid and an isotropic liquid phase, but did not show any thermotropic liquid crystalline behavior. This is reflected in a single phase-transition of considerable enthalpy in the DSC thermograms. The optical polarizing images of cooled isotropic liquids are more in line with a gel phase than a crystal. However, the DSC, as depicted in Figure 6, revealed no phase transition upon cooling. Instead an exothermic peak was observed closely before the melting. This indicates a kinetically hindered crystallization and, therefore, identifies the low temperature phase as a crystalline solid. Interestingly all compounds exhibited practically identical phase transition data, as shown in Table 2. This suggests that the crystallization is entirely driven by the hydrophilic domain. Compared to previously reported isosteric esters[26,27] the diamides **9** exhibit higher melting temperatures, probably reflecting intermolecular hydrogen bonding involving the amides.

The mono-antennary surfactant type **15**, on the other hand, did not show a reversible phase transition from a solid to a liquid phase. A phase transition could only be observed for the first heating cycle. The longer chained lipids **15b** and **15c** turned into liquid phase at about 190 °C, but the transition coincides with significant degradation. The latter may be a reason for the non-reversible melting process. However, no indication of degradation was observed in the DSC of **15a**, as depicted in Figure 7. Here the reformation of a solid phase appears to be too strongly kinetically hindered for a DSC observation. A closer look revealed two transitions at 183 and 185 °C with enthalpies of 16 and 37 J g^{-1}, referring to 8 and 19 KJ mol^{-1}, respectively. The two phase-transitions may refer to the different diastereomers of **15a**, due to the non-symmetric tetrahydro-pyrimidine ring. Although the ratio of the enthalpies does not match the diastereomeric composition of about 4:1 according to NMR, the close proximity of the phase transitions may be responsible for inaccurate enthalpy values.

In contact with water the bi-antennary glycolipids of structure type **9** exhibited particularly the hexagonal phase H_I. Besides this dominating lyotropic phase, the optical polarizing (OPM) image of **9a** in Figure 8 shows a narrow 'black' band followed by another unspecific birefrigent texture on the low water concentration side. These reflect the bicontinuous cubic phase Q_I and the lamellar

† Additional modeling views are available in Supplementary data.

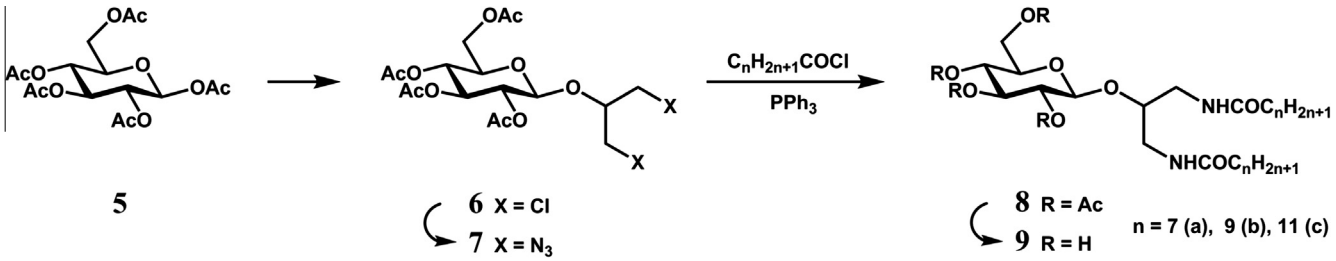

Figure 2. Synthesis of bi-antennary amide linked glycolipids from glucose.

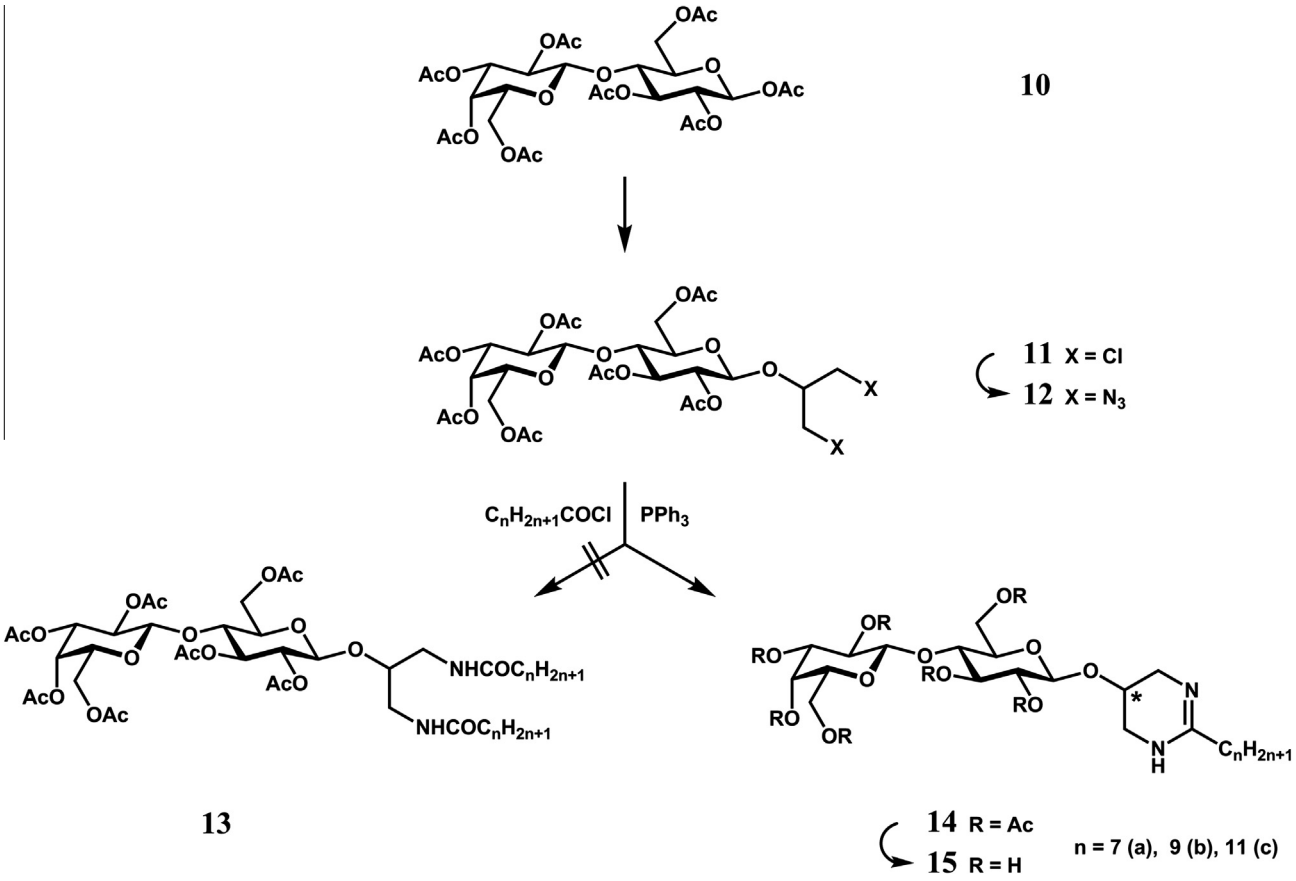

Figure 3. Staudinger reaction of lactose based diazides with fatty acids.

phase L_{α}. The contact penetration scan suggests a rather small concentration range for these two phases. The phase sequence is consistent with the packing theory.[12] For higher homologs the lyotropic texture is significantly reduced in size, thus less clear. The reason is the low water solubility of the surfactants, which is reflected in the high Krafft temperatures particularly of **9b** and **9c**, as shown in Table 3.

The mono-antennary surfactants of type **15** exhibited significantly lower Krafft temperatures. This is expected based on the reduced size of the overall hydrophilic domain. However, the Kraft temperatures are comparably high, thus indicating strong intermolecular interactions. It is expected that hydrogen bonds involving the tetrahydro-pyrimidine NH are contributing considerably. In contact with water only a hexagonal H_I phase was observed. This reflects a significantly larger molecular surface area for the hydrated sugar compared to the single alkyl chain. The absence of an anisotropic phase for the C_7 chained surfactant **15a** can be explained with its high solubility. The CMC of the C_{11}-surfactant **15c** was determined at 60 °C as 0.41 mmol L^{-1}, see Figure 9. This value is in agreement with those for other surfactants of similar chain length. The correlated surface tension of 29 mN m^{-1} suggests a good emulsifying ability.

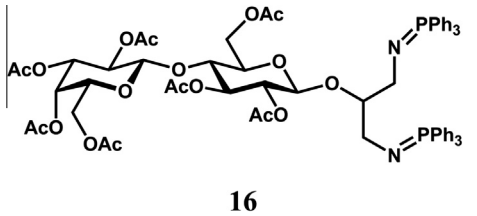

Figure 4. Structure of the Staudinger bis-iminophosphorane intermediate.

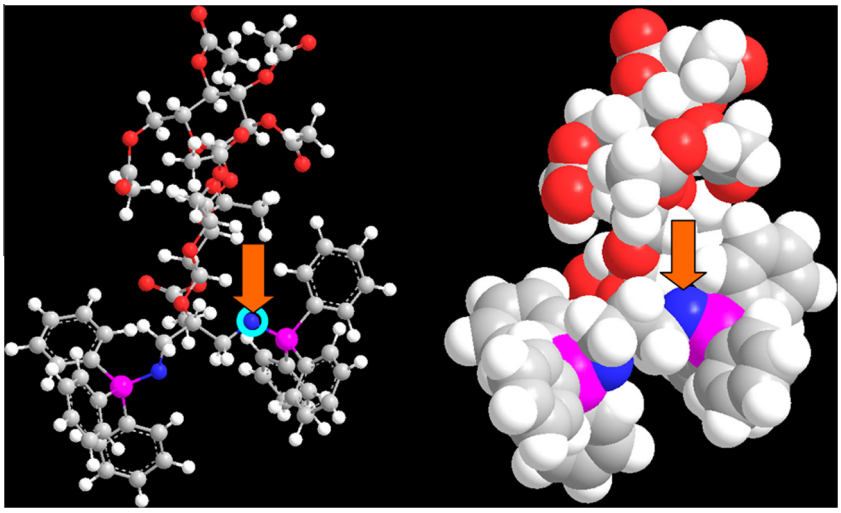

Figure 5. Steric hindrance by non-reducing galactose unit blocks fatty acid access to one iminophorphorane.

Table 1
Diastereomeric excess for compounds **14** and **15**

Compds	Chain length	de (%)
14a, 15a	C_7H_{15}	60
14b, 15b	C_9H_{19}	20
14c, 15c	$C_{11}H_{23}$	50

Table 2
Thermo-analytical data for biantennary surfactants **9**

Compds	Mp (°C)	ΔH (kJ mol^{-1})
9a	119	19
9b	120	23
9c	119	22

3. Conclusion

A synthetic approach to new glycolipids has been developed. The Staudinger reaction enables an easy access to diamide linked bi-antennary surfactants with close structural similarity to natural glycol-glycerolipids, provided the diazidoalkyl glycoside intermediate does not give rise to steric hindrance. In case of the latter, an intra-molecular cyclization of a monoamide leads to a tetrahydropyrimidine linked mono-antennary surfactant instead. It is expected that the cyclization may be promoted for starting materials without steric hindrance, if only one equivalent of fatty acid chloride is applied in the coupling. However, the efficiency of such a reaction remains to be investigated.

Amide analogs of glycol-glycero lipids exhibit very high Krafft temperatures. This may affect their potential use in a vesicular delivery system, as formulations require high temperature treatments. On the other hand, the expression of a bicontinuous cubic phase in contact with water is a promising indication for the target

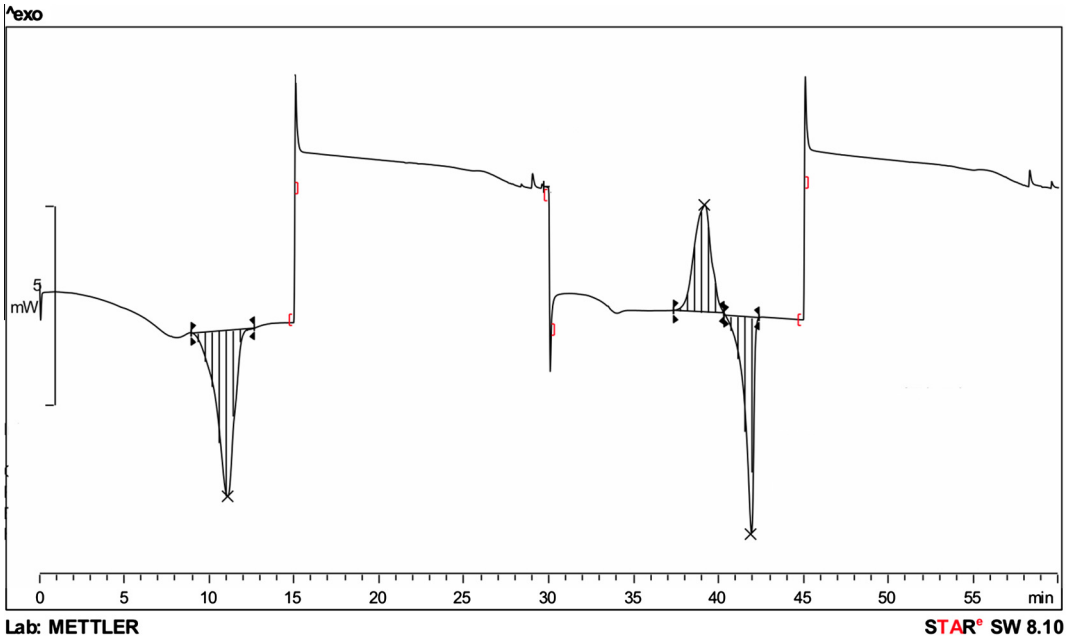

Figure 6. DSC thermogram for **9c** in two heating–cooling cycles.

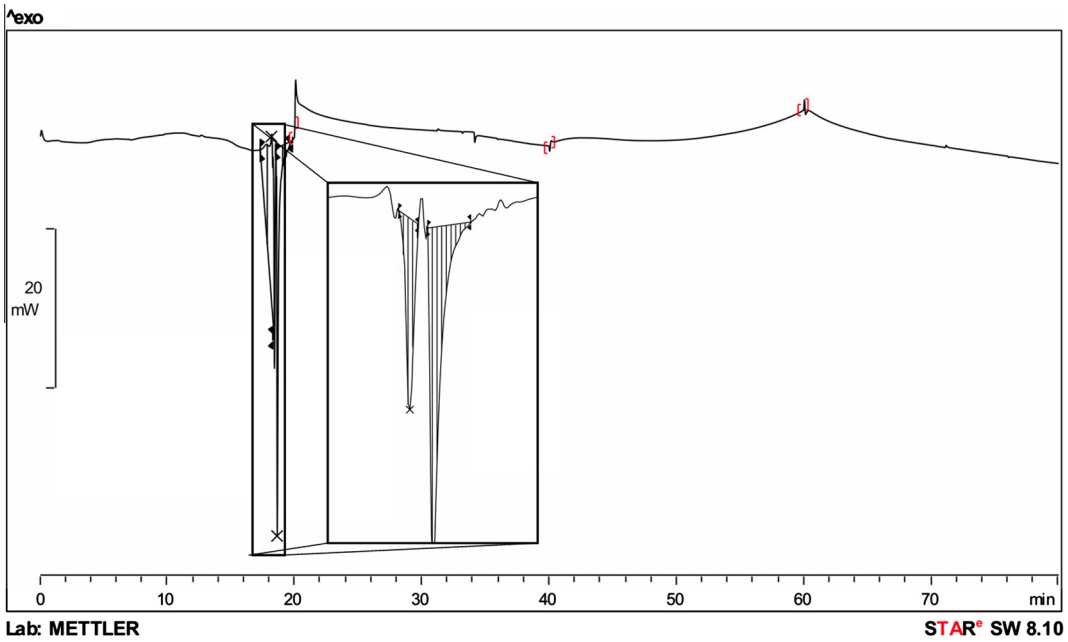

Figure 7. DSC thermogram for **15a** in two heating–cooling cycles.

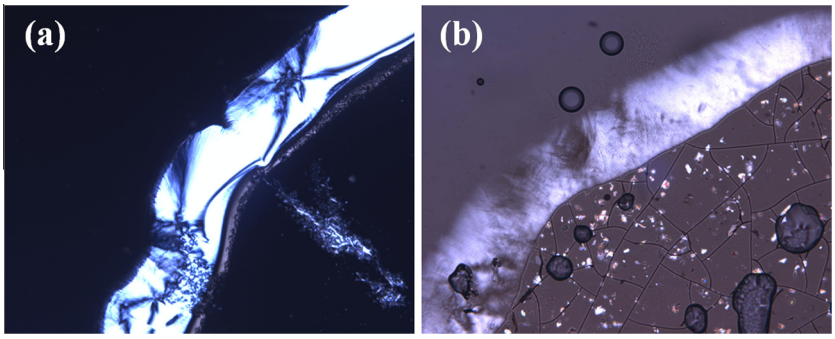

Figure 8. Water contact penetration scans for **9a** (a) and **15b** (b), respectively; the water concentration increases from left to right.

Table 3
Selected surfactant data for mono- and bi-antennary glycolipids **9** and **15**

Compds	T_K (°C)	Phases with water
9a	75	L_α, Q_I, H_I
9b	85	$L_\alpha/(H_I)$
9c	95	$L_\alpha/(H_I)$
15a	45	L_1
15b	50	H_I
15c	55	H_I

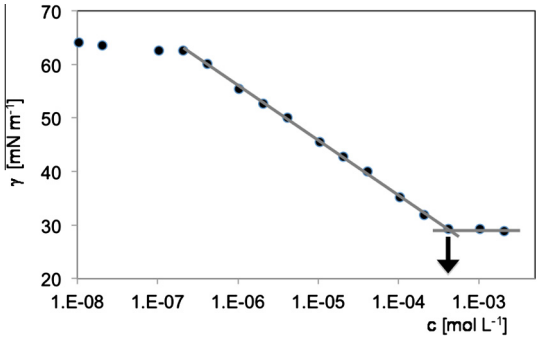

Figure 9. Surface tension based CMC determination for **15c**.

application, as this phase plays a key role in the fusion of a vesicle with a cellular membrane.[28–30]

4. Experimental

4.1. General methods

Melting temperatures were determined using a manual melting point apparatus and are uncorrected. Optical rotations were measured at 589 nm in 10 cm cells at room temperature. NMR spectra were recorded on Jeol and Bruker spectrometers at 400 MHz for ^{1}H and 100 MHz for ^{13}C, respectively. Assignments of ^{13}C-signals are based on HMQC spectra. High-resolution mass spectra were recorded on an LC–MS system, applying MeOH/water eluents. Phase-transition temperatures were determined by DSC in replicated heating–cooling cycles at a heating/cooling rate of 10 °C min^{-1}. Lyotropic phases were investigated using the contact

penetration technique under OPM observation.[32,33] The determination of Krafft points applied heating 20 mL samples of the surfactant in water at a concentration of about 10% above the CMC in an oil bath under moderate stirring until the mixture cleared. Critical micelle concentrations were determined by surface tension measurements. The intersection of the concentration dependent and the high concentration independent region in the plot of the surface tension versus the logarithmic concentration determines the CMC. Surface tension measurements were measured at rt in 5 replicates with a standard deviation below 0.1 mN m^{-1}.

4.1.1. Glycosylation

Sugar β-peracetate (5 mmol) and 1,3-dichloro-2-propanol (6 mmol) were dissolved in anhydr. CH_2Cl_2 (50 mL) and treated with $BF_3 \times Et_2O$ (6 mmol). The reaction mixture was kept for about 3 h at rt before it was quenched with water. The organic layer was separated, washed with water and aqueous $NaHCO_3$, dried over $MgSO_4$, and concentrated. The crude product was purified by crystallization from EtOH to provide **6** and **11**, respectively, in about 50% yield.

4.1.2. Substitution to introduce azides

A solution of 1,3-dichloro-propylglycoside **6** or **11** (1 mmol) in DMF (25 mL) was treated with NaN_3 (6 mmol) and the suspension was heated to 80 °C for 24 h. After cooling to rt the reaction mixture was diluted with water and extracted with CH_2Cl_2. The organic layer extract was washed with water and aqueous $NaHCO_3$, dried over $MgSO_4$ and concentrated. Recrystallization of the crude product from ethanol furnished **7** and **12**, respectively, in about 75% yield.

4.1.3. Staudinger reaction

To a solution of the diazide (2 mmol) in CH_2Cl_2 (25 mL, 40 mL for the disaccharide based diazide) was added triphenylphosphine (1.25 g, 4.8 mmol). After the gas evolution has ceased a solution of the acid chloride (6.4 mmol) in CH_2Cl_2 (5 mL) was added drop-wise at rt. The reaction was left to stir at rt for 7–15 h, by which it had become cloudy. The solid was removed by filtration and the solution was washed with aqueous $NaHCO_3$ and dried over $MgSO_4$. After removal of the solvent the crude product was purified by chromatography on silica using ethyl acetate and acetone 6:1.

4.1.4. Deacetylation

The carbohydrate was dissolved in MeOH and treated with a catalytic amount of NaOMe. The reaction was left to complete over night at rt, before neutralization with Amberlite 120 (H^+). The resin was filtered off and the solvent was evaporated to provide the surfactants in practical quantitative yield.

4.2. 1,3-Dioctanamido-2-propyl-β-D-glucopyranoside (9a)

4.2.1. 1,3-Dioctanamido-2-propyl 2,3,4,6-tetra-*O*-acetyl-β-D-glucopyranoside (8a)

Compound **7** (1.5 g, 3.17 mmol) was coupled with octonyl chloride according to the procedure 4.1.3 to yield 1.4 g, (63%) of compound **8a** as white crystals. Mp 76 °C. $[\alpha]_D^{25}$ −45 (*c* 0.15, $CHCl_3$). ^1H NMR (400 MHz, $CDCl_3$) δ = 6.58, 6.19 (2 t, 2H, NH), 5.18 (dd∼t, H-3), 5.04 (dd∼t, H-4), 4.95 (dd, H-2), 4.60 (d, H-1), 4.23 (dd, H-6A), 4.20 (dd, H-6B), 3.81–3.66 (m, 4H, H-5, CH, 2 NCH_2-A), 3.05 (ddd∼dt, NCH_2-B), 2.67 (ddd, NCH_2-B), 2.21, 2.18 (2 t, 2 × 2H, α-CH_2), 2.07, 2.04, 2.03, 1.99 (4 s, 4 × 3H, Ac), 1.61 (m_c, 4H, β-CH_2), 1.27 (m_c, 16H, bulk-CH_2), 0.86 (2 t, 2 × 3H, CH_3); $^3J_{1,2}$ = 8.0, $^3J_{2,3}$ = 9.5, $^3J_{3,4}$ = 9.5, $^3J_{4,5}$ = 10.0, $^3J_{5,6A}$ = 2.5, $^3J_{5,6B}$ = 4.5, $^2J_6$ = 12.0, $^3J_{CH2,CH}$ = 5.0, $^3J_{CH2,NH}$ = 5.0, $^2J_{CH2}$ = 15.0, $^3J_{CH2,CH}$ = 8.0, $^3J_{CH2,NH}$ = 5.0, $^2J_{CH2}$ = 15.0 Hz. ^{13}C NMR (100 MHz, $CDCl_3$) δ = 175.34, 174.52 (CONH), 171.17, 170.57,170.05, 169.97 (COO), 100.90 (C-1), 77.76 (CH), 72.45 (C-3), 72.01 (C-5), 71.15 (C-2), 68.13 (C-4), 61.52 (C-6), 39.62, 38.62 (CH_2N), 36.49, 36.34 (α), 31.40 (2 ω-2), 28.97 (2), 28.69 (2) (bulk-CH_2), 25.48, 25.37 (β), 22.37 (ω-1), 20.44, 20.39, 20.26 (2) (Ac), 13.69 (ω). Elemental analysis for $C_{33}H_{56}N_2O_{12}$: C, 58.91; H, 8.39; N, 4.16, found: C, 57.54; H, 8.85; N, 3.87; matching monohydrate $C_{33}H_{56}N_2O_{12} \times H_2O$, calcd: C, 57.37; H, 8.46; N, 4.06.

4.2.2. 1,3-Dioctanamido-2-propyl-β-D-glucopyranoside (9a)

Compound **8a** (1.25 g, 1.82 mmol) was deacetylated according to the procedure 4.1.4 to give (0.87 g, 95%) of compound **9a**. Mp 119 °C. $[\alpha]_D^{25}$ −3.0 (*c* 0.15, CH_3OH). ^1H NMR (400 MHz, CD_3OD) δ = 7.95, 7.81 (2 t, NH), 4.36 (d, H-1), 3.89 (dd, H-6A), 3.80 (mc, OCH), 3.70 (dd, H-6B), 3.49–3.22 (m, 7H, H-3, H-4, H-5, CH_2N), 3.21 (dd, H-2), 2.22, 2.21 (2 t, 4H, α-CH_2), 1.60 (m_c, 4H, β-CH_2), 1.31 (mc, 16H, bulk-CH_2), 0.90 (t, 6H, CH_3); $^3J_{1,2}$ = 8.0, $^3J_{2,3}$ = 9.0, $^3J_{5,6A}$ = 2.0, $^3J_{5,6B}$ =5.5, $^2J_6$ = 12.0 Hz. ^{13}C NMR (100 MHz, CD_3OD) δ = 175.35 (2 CONH), 104.87 (C-1), 79.80 (CH), 78.24, 78.10 *(C-3 & C-5)*, 75.34 (C-2), 71.69 *(C-4)*, 62.81 (C-6), 42.68, 41.99 (CH_2N), 37.21, 37.09 (α), 32.87 (2 ω-2), 30.27 (2), 30.12, 30.10 (bulk-CH_2), 26.96, 26.91 (β), 23.60 (2 ω-1), 14.29 (2 ω). HRMS: $[M+H]^+$ calcd for $C_{25}H_{49}N_2O_8$: 505.3489, 506.3522 (28%), found: 505.3480 (100%), 506.3505 (31%); $[M+Na]^+$ calcd for $C_{25}H_{48}N_2O_8Na$: 527.3313, 528.3339 (28%), found: 527.3313 (100%) 528.3339 (29%).

4.3. 1,3-Didecanamido-2-propyl-β-D-glucopyranoside (9b)

4.3.1. 1,3-Didecanamido-2-propyl 2,3,4,6-tetra-*O*-acetyl-β-D-glucopyranoside (8b)

Compound **7** (1.5 g, 3.17 mmol) was coupled with decanoyl chloride according to the procedure 4.1.3 to provide 1.5 g, (62%) of compound **8b** as white crystals. Mp 80 °C. $[\alpha]_D^{25}$ −39 (*c* 0.15, $CHCl_3$). ^1H NMR (400 MHz, $CDCl_3$) δ = 6.56, 6.17 (2 t, 2H, NH), 5.19 (dd∼t, H-3), 5.05 (dd∼t, H-4), 4.95 (dd, H-2), 4.61 (d, H-1), 4.23 (dd, H-6A), 4.18 (dd, H-6B), 3.82–3.66 (m, 4H, H-5, CH, 2 CH_2N-A), 3.05 (m_c, CH_2N-B), 2.67 (m_c, CH_2N-B), 2.21, 2.18 (2 t, 2 × 2H, α−CH2), 2.08, 2.05, 2.03, 2.00 (4 s, 4 × 3H, Ac), 1.61 (mc, 4H, β-CH_2), 1.32–1.20 (m, 24H, bulk-CH_2), 0.86 (t, 6H, CH_3); $^3J_{1,2}$ = 8.0, $^3J_{2,3}$ = 9.5, $^3J_{3,4}$ = 9.5, $^3J_{4,5}$ = 10.0, $^3J_{5,6A}$ = 2.5, $^3J_{5,6B}$ = 4.5, $^2J_6$ = 12.5 Hz. ^{13}C NMR (100 MHz, $CDCl_3$) δ = 175.34 (CONH), 171.17, 170.58, 170.05, 169.98 (COO), 100.92 (C-1), 77.80 (CH), 72.46 (C-3), 72.04 (C-5), 71.17 (C-2), 68.15 (C-4), 61.53 (C-6), 39.61, 38.61 (CH_2N), 36.52, 36.38 (α), 31.59 (2 ω-2), 29.17 (2), 29.05 (4), 28.99 (4) (bulk-CH_2), 25.49, 25.39 (β), 22.35 (2 ω-1), 20.45, 20.40, 20.27 (2) (Ac), 13.75 (2 CH_3). Elemental analysis for $C_{37}H_{64}N_2O_{12}$: C, 60.97; H, 8.85; N, 3.84, found: C, 60.18; H, 9.27; N, 3.69; matching hemihydrate $C_{37}H_{64}N_2O_{12} \times ½\ H_2O$, calcd: 60.22, H, 8.88; N, 3.80.

4.3.2. 1,3-Didecanamido-2-propyl-β-D-glucopyranoside (9b)

Compound **8b** (1.25 g, 1.71 mmol) was deacetylated according to the procedure 4.1.4 to yield (0.93 g, 96%) of compound **9b**. Mp 120 °C. $[\alpha]_D^{25}$ −4.0 (*c* 0.15, CH_3OH). ^1H NMR (400 MHz, CD_3OD) δ = 7.94, 7.81 (2 t, NH), 4.37 (d, H-1), 3.89 (dd, H-6A), 3.80 (mc, OCH), 3.67 (dd, H-6B), 3.49–3.24 (m, 7H, H-3, H-4, H-5, CH_2N), 3.21 (dd, H-2), 2.23, 2.21 (2 t, 4H, α-CH_2), 1.60 (m_c∼br s, 4H, β-CH_2), 1.30 (m_c∼br s, 24H, bulk-CH_2), 0.90 (t, 6H, CH_3); $^3J_{1,2}$ = 8.0, $^3J_{2,3}$ = 9.0, $^3J_{5,6B}$ = 5.0, $^2J_6$ = 11.5 Hz. ^{13}C NMR (100 MHz, CD_3OD) δ = 175.35 (2 CONH), 104.87 (C-1), 79.80 (CH), 78.24, 78.11 *(C-3 & C-5)*, 75.35 (C-2), 71.69 *(C-4)*, 62.82 (C-6), 42.67, 41.98 (CH_2N), 37.21, 37.10 (α), 33.01 (2 ω-1), 30.58 (2), 30.46, 30.43, 30.38 (2), 30.31 (2) (bulk-CH_2), 26.96, 26.91 (β), 23.65 (2 ω-1), 14.32 (2 ω). HRMS: $[M+H]^+$ calcd for $C_{29}H_{57}N_2O_8$: 561.4115, 562.4148 (32%), found: 561.4107, 562.4138 (31%); $[M+Na]^+$ calcd for $C_{29}H_{56}N_2O_8$-Na: 583.3934, found: 583.3909 (very weak).

4.4. 1,3-Didodecanamido-2-propyl-β-D-glucopyranoside (9c)

4.4.1. 1,3-Didodecanamido-2-propyl 2,3,4,6-tetra-*O*-acetyl-β-D-glucopyranoside (8c)

Compound **7** (1.5 g, 3.17 mmol) was coupled with dodecanoyl chloride according to the procedure 4.1.3 to yield 1.6 g, (60%) of compound **8c** as white crystals. Mp 86 °C. $[\alpha]_D^{25}$ −35 (*c* 0.15, $CHCl_3$). ^1H NMR (400 MHz, $CDCl_3$) δ = 6.57, 6.18 (2 t, 2H, NH), 5.18 (dd∼t, H-3), 5.04 (dd∼t, H-4), 4.95 (dd, H-2), 4.60 (d, H-1), 4.23 (dd, H-6A), 4.18 (dd, H-6B), 3.81–3.60 (m, 4H, H-5, OCH, 2 CH_2N), 3.05 (ddd∼dt, CH_2N-B), 2.67 (ddd, CH_2N-B), 2.21, 2.18 (2 t, 2 × 2H, α), 2.07, 2.04, 2.02, 1.99 (4 s, 4 × 3H, Ac), 1.60 (m_c, 4H, β), 1.31–1.21 (m, 32H, bulk-CH_2), 0.86 (t, 6H, CH_3); $^3J_{1,2}$ = 8.0, $^3J_{2,3}$ = 9.5, $^3J_{3,4}$ = 9.5, $^3J_{4,5}$ = 10.0, $^3J_{5,6A}$ = 2.5, $^3J_{5,6B}$ = 5.0, $^2J_6$ = 12.5, $^3J_{CH2,CH}$ = 5.0, $^3J_{CH2,NH}$ = 5.0, $^2J_{CH2}$ = 15.0, $^3J_{CH2,CH}$ = 8.0, $^3J_{CH2,NH}$ = 5.0, $^2J_{CH2}$ = 15.0 Hz. ^{13}C NMR(100 MHz, $CDCl_3$) δ = 175.33, 174.50 (CONH), 171.15, 170.56, 170.03, 169.96 (COO), 100.89 (C-1), 77.76 (CH), 72.44 (C-3), 72.01 (C-5), 71.14 (C-2), 68.13 (C-4), 61.51 (C-6), 39.60, 38.61 (CH_2N), 36.49, 36.34 (α), 31.63 (2 ω-2), 29.32 (4), 29.21 (2), 29.04 (6) (bulk-CH_2), 25.48, 25.37 (β), 22.35 (2 ω-1), 20.43, 20.38, 20.25 (2) (Ac), 13.74 (2 CH_3). Elemental analysis for $C_{41}H_{72}N_2O_{12}$: C, 62.73; H, 9.24; N, 3.57, found: C, 62.47; H, 9.68; N, 3.39.

4.4.2. 1,3-Didodecanamido-2-propyl-β-D-glucopyranoside (9c)

Compound **8c** (1.5 g, 1.91 mmol) was deacetylated according to the procedure 4.1.4 to furnish 1.1 g, (93%) of compound **9c**. Mp 119 °C. $[\alpha]_D^{25}$ −6.0 (*c* 0.15, CH_3OH). ^1H NMR (400 MHz, CD_3OD) δ = 7.95, 7.81 (2 t, NH), 4.37 (d, H-1), 3.89 (dd, H-6A), 3.80 (mc, OCH), 3.67 (dd, H-6B), 3.49–3.24 (m, 7H, H-3, H-4, H-5, CH_2N), 3.21 (dd, H-2), 2.23, 2.21 (2 t, 4H, α-CH_2), 1.62 (m_c, 4H, β-CH_2), 1.36–1.26 (m, 32H, bulk-CH_2), 0.90 (t, 6H, CH_3); $^3J_{1,2}$ = 8.0, $^3J_{2,3}$ = 9.0, $^3J_{5,6A}$ = 1.5, $^3J_{5,6B}$ =5.0, $^2J_6$ = 11.5 Hz. ^{13}C NMR (100 MHz, CD_3OD) δ = 177.32 (2 CONH), 104.85 (C-1), 79.78 (CH), 78.25, 78.11 *(C-3 & C-5)*, 75.35 (C-2), 71.70 *(C-4)*, 62.82 (C-6), 42.68, 41.97 (CH_2N), 37.22, 37.11 (α), 33.05 (2, ω-2), 30.72 (4), 30.63 (2), 30.44 (4), 30.32 (2) (bulk-CH_2), 26.97, 26.92 (β), 23.66 (2 ω-1), 14.32 (2 ω). HRMS: $[M+H]^+$ calcd for $C_{33}H_{65}N_2O_8$: 617.4741, 618.4774 (37%), found: 617.4739 (100%), 618.4763 (36%).

4.5. 2-Heptyl-5-(4-*O*-β-D-galactopyranosyl-β-D-glucopyranosyl)-1,4,5,6-tetrahydro-pyrimidine (15a)

4.5.1. 2-Heptyl-5-(2,3,4,2′,3′.4′,6′-hepta-*O*-acetyl-β-lactosyl)-1,4,5,6 tetrahydropyrimidine (14a)

Compound **13** (1 g, 1.31 mmol) was coupled with octanoyl chloride according to the procedure 4.1.3 to yield 0.75 g, (70%) of compound **14a** as white crystals. Mp 188 °C. $[\alpha]_D^{25}$ +21.0 (*c* 0.15, $CHCl_3$). ^1H NMR (400 MHz, $CDCl_3$) δ = 6.11, 5.72 (2 dd∼t, 1H, 1:4, NH), 5.32 (dd∼d, H-4′), 5.17 (dd∼t, H-3), 5.08 (dd, H-2′), 4.92 (dd, H-3′), 4.87 (dd, H-2), 4.61, 4.46 (2 d, 2 × 1H, H-1, H-1′), 4.49 (dd∼d, H-6/6′), 4.15–4.01 (m, 3H, H-6/6′), 3.91 (m_c, CH), 3.85 (m_c, H-5/5′), 3.74 (dd∼t, H-4), 3.67–3.25 (m, 5H, H-5, CH_2), 2.13, 2.09, 2.04 (2), 2.03 (2), 1.94 (7 s, 21H, Ac), 1.86 (m_c, 2H, α-CH_2), 1.59 (m_c, 2H, β-CH_2), 1.26 (m_c, 8H, bulk-CH_2), 0.85 (t, 3H, CH_3); $^3J_{1,2}$ = 8.0, $^3J_{2,3}$ = 9.0, $^3J_{3,4}$ = 9.0, $^3J_{4,5}$ = 9.0, $^3J_{1',2'}$ = 8.0, $^3J_{2',3'}$ = 10.0, $^3J_{3',4'}$ = 3.0, $^3J_{4',5'}$ ⩽1 Hz. ^{13}C NMR(100 MHz, $CDCl_3$) δ = 174.03 (C═N), 170.92, 170.90, 170.68, 170.63, 170.26, 170.22, 169.60 (C═O), 101.22, (101.10), 100.68 (C-1, C-1′), 79.00 (CH), 76.13 (C-4), 72.83 (C-5), 72.60 (C-3), 71.91 (C-2), 70.86 (C-3′), 70.68 (C-5′), 69.02 (C-2′), 66.51 (C-4′), 61.57, 60.68 (C-6, C-6′), (44.68), 43.82 (CH_2N), (41.29), 40.54 (CH_2NH), 36.37 (α), 31.38 (ω-2), 28.97, 28.67 (bulk-CH_2), 25.31 (β), 22.24 (ω-1), 20.45, 20.41, 20.27 (4), 20.14 (Ac), 13.65 (ω). Elemental analysis for $C_{37}H_{56}N_2O_{18}$: C, 54.40; H, 6.91; N, 3.43, found: C, 53.54; H, 7.17; N, 3.47.

4.5.2. 2-Heptyl-5-β-lactosyl-1,4,5,6-tetrahydropyrimidine (15a)

Compound **14a** (0.5 g, 0.61 mmol) was deacetylated according to the procedure 4.1.4 to furnish (0.3 g, 94%) of anomeric mixture of compound **15a**. Mp 183–185 °C. $[\alpha]_D^{25}$ +5.0 (*c* 0.15, CH_3OH). ^1H NMR (400 MHz, CD_3OD) δ = (4.48)/4.45, 4.36/(4.35) (2 × 2 d, 2H, H-1, H-1′), 4.02–3.25 (m, 17H), (2.38)/2.21 (m_c, 2H, α-CH_2), 1.61 (m_c, 2H, β-CH_2), 1.32 (m_c, 8H, bulk-CH_2), 0.90 (t, 3H, CH_3); $^3J_{1,2}$ = 8.0/7.5, $^3J_{1',2'}$ = 7.5/8.0 Hz. ^{13}C NMR (100 MHz, CD_3OD) δ = 177.50 (C═N), 105.51, 105.33 (C-1, C-1′), 80.71, 80.28, 77.30, 76.81, 76.46, 75.02 (2), 72.73, 70.48, 62.63, 61.96 (C-6, C-6′), 45.50 (CH_2N), 41.59 (CH_2NH), 37.14 (α), 32.84 (ω-2), 30.23, 30.05 (bulk-CH_2), 26.86 (β), 23.55 (ω-1), 14.24 (ω).

4.6. 2-Nonyl-5-(4-*O*-β-D-galactopyranosyl-β-D-glucopyranosyl)-1,4,5,6-tetrahydro-pyrimidine (15b)

4.6.1. 2-Nonyl-5-(2,3,4,2′,3′.4′,6′-hepta-*O*-acetyl-β-lactosyl)-1,4,5,6-tetrahydropyrimidine (14b)

Compound **13** (1 g, 1.31 mmol) was coupled with decanoyl chloride according to the procedure 4.1.3 to produce 0.78 g, (70%) of compound **14b** as white crystals. Mp 195 °C. $[\alpha]_D^{25}$ +10.0 (*c* 0.15, $CHCl_3$). ^1H NMR (400 MHz, $CDCl_3$) δ = 5.98, 5.59 (2 dd∼t, 1H, 2:3, NH), 5.20 (dd∼d, H-4′), (5.08)/(5.05 (dd∼t, H-3), (4.98)/4.96 (dd, H-2′), (4.83)/4.82 (dd, H-3′), (4.78)/4.75 (dd, H-2), 4.49/(4.44), (4.37)/4.34 (2 d, H-1, H-1′), 4.38 (dd, H-6/6′A), 3.99 (dd, H-6′/6A), 3.95 (dd, H6/6′B), 3.92 (dd, H-6′/6B), 3.82–3.66 (m, 2H, CH, H-5′), 3.62 (dd∼t, H-4), 3.54–3.14 (m, 5H, H-5, CH_2N), 2.01 (2), 1.98 (2), 1.92, 1.91 (2), 1.90, 1.82, 1.82 (Ac), 1.55 (m_c, 2H, α-CH_2), 1.46, m_c, 2H, β-CH_2), 1.18–1.09 (m, 12H, bulk-CH_2), 0.73 (t, 3H, CH_3); $^3J_{1,2}$ = 8.0, $^3J_{2,3}$ = 10.0, $^3J_{3,4}$ = 9.5, $^3J_{4,5}$ = 9.5, $^3J_{1',2'}$ = 8.0, $^3J_{2',3'}$ = 10.0, $^3J_{3',4'}$ = 3.0, $^3J_{4',5'}$ ⩽1, $^3J_{5/5',6/6'A}$ = 2.0, $^3J_{5/5',6/6'B}$ = 7.0, $^2J_{6/6'}$ = 11.5, $^3J_{5'/5,6'/6A}$ = 6.0, $^3J_{5'/5,6'/6B}$ = 7.5, $^2J_{6/6'}$ = 11.5 Hz. ^{13}C NMR (100 MHz, $CDCl_3$) δ 174.21, 173.99 (C═N), 170.92, 170.89, 170.68, 170.63, 170.38, 170.26, 170.22, 170.17, 169.60, 169.55 (C═O), 101.25, 101.23, 101.10, 100.66 (C-1, C-1′), 80.89, 78.99 (CH), 76.13, 75.81 (C-4), 73.02, 72.81 (C-3), 72.59 (C-3′), 72.27, 71.90 (C-2), 71.21, 70.85 (C-3′), 70.67 (C-5′), 69.06, 69.01 (C-2′), 66.50 (C-4′), 61.56, 61.33, 60.67, 60.64 (C-6, C-6′), 44.65, 43.80 (CH_2N), 41.24, 40.50 (CH_2NH), 36.35, 36.13 (α), 31.55 (ω-2), 29.15, 29.13, 29.07, 29.03, 28.97, 28.94 (bulk-CH_2), 25.33, 25.31 (β), 22.30 (ω-1), 20.51, 20.44, 20.41, 20.38, 20.28, 20.15 (Ac), 13.70 (ω). Elemental analysis for $C_{39}H_{60}N_2O_{18}$: C, 55.44; H, 7.16; N, 3.32, found: C, 55.72; H, 7.26; N, 3.72.

4.6.2. 2-Nonyl-5-β-lactosyl-1,4,5,6-tetrahydropyrimidine (15b)

Compound **14b** (0.5 g, 0.58 mmol) was deacetylated according to the procedure 4.1.4 to furnish (0.3 g. 94%) of compound **15b**. Mp 190 °C (dec). $[\alpha]_D^{25}$ +15.0 (*c* 0.15, CH_3OH). ^1H NMR (400 MHz, CD_3OD) δ = 4.47/4.45, 4.36/4.35 (2 × 2 d, 2H, H-1 & H-1′), 4.04–3.25 (m, 17H), 2.21 (m_c, 2H, α-CH_2), 1.61 (m_c, 2H, β-CH_2), 1.31 (m_c, 12H, bulk-CH_2), 0.90 (t, 3H, CH_3); $^3J_{1,2}$ = 8.0/7.5, $^3J_{1',2'}$ = 7.5/8.0 Hz. ^{13}C NMR(100 MHz, CD_3OD) δ = 177.49 (C═N), 105.52, 105.35/(104.20) (C-1, C-1′), (80.80)/80.75, 80.28/(79.49), 77.32, 76.82, 76.52/(76.47), 75.06 (2)/(74.88), 72.75, 70.49, 62.63, (62.06)/62.01 (C-6, C-6′), 45.50/(45.04) (CH_2N), (42.65)/41.62 (CH_2NH), 37.15/(37.03) (α), 32.97 (ω-2), 30.54, 30.38, (30.40), 30.32, 30.28 (bulk-CH_2), (26.89)/26.86 (β), 23.60 (ω-1), 14.25 (ω).

4.7. 2-Undecyl-5-(4-O-β-D-galactopyranosyl-β-D-glucopyranosyl)-1,4,5,6-tetrahydro-pyrimidine (15c)

4.7.1. 2-Undecyl-5-(2,3,4–2′,3′.4′,6′-hepta-O-acetyl-β-lactosyl)-1,4,5,6-tetrahydropyrimidine (14c)

Compound **13** (1 g, 1.31 mmol) was coupled with dodecanoyl chloride according to the procedure 4.1.3 to produce (0.82 g,

70%) of compound **14c** as white crystals. Mp 199 °C. $[\alpha]_D^{25}$ +8.0 (*c* 0.15, $CHCl_3$). ^{1}H NMR (400 MHz, $CDCl_3$) δ = 5.99, 5.61 (2 dd∼t, 1H, 1:3, NH), 5.21 (dd∼d, H-4′), (5.08)/5.05 (dd∼t, H-3), (4.98)/4.97 (dd, H-2′), (4.83)/4,82 (dd, H-3′), 4.76 (dd, H-2), 4.49/(4.45), (4.38)/4.35 (2 d, H-1, H-1′), 4.39 (dd, H-6/6′A), 4.00 (dd, H-6′/6A), 3.96 (dd, H-6/6′B), 3.93 (dd, H-6′/6B), 3.80 (m_c, CH), 3.74 (ddd∼t, H-5′), 3.63 (dd∼t, H-4), 3.51 (dd, CH_2N-A), 3.41 (dd, CH_2N-B), 3.51–3.27 (m, 2H, H-5, CH_2NH-A), 3.20 (ddd∼dt, CH_2NH-B), 2.02, 1.98, 1.93, 1.92 (2), 1.91, 1.83 (7 s, 21H, Ac), 1.64 (m_c, 2H, α-CH_2), 1.47 (m_c, 2H, β-CH_2), 1.18–1.08 (m, 16H, bulk-CH_2), 0.74 (t, 3H, CH_3); $^3J_{1,2}$ = 8.0, $^3J_{2,3}$ = 9.5, $^3J_{3,4}$ = 10.0, $^3J_{4,5}$ = 9.5, $^3J_{1',2'}$ = 8.0, $^3J_{2',3'}$ = 10.0, $^3J_{3',4'}$ = 3.0, $^3J_{4',5'} \leqslant 1$, $^3J_{5/5',6/6'A}$ = 1.0, $^3J_{5/5',6/6'B}$ = 7.0, $^2J_{6/6'}$ = 11.5, $^3J_{5'/5,6'/6A}$ = 6.0, $^3J_{5'/5,6'/6B}$ = 7.5, $^2J_{6/6'}$ = 11.0, $^3J_{CH,CH2N\text{-}A}$ = 4.0, $^3J_{CH,CH2N\text{-}B}$ = 6.0, $^2J_{CH2N}$ = 12.0, $^3J_{CH,CH2NH\text{-}B}$ = 7.5, $^3J_{NH,CH2NH\text{-}B}$ = 6.0, $^2J_{CH2NH}$ = 14.0 Hz. ^{13}C NMR (100 MHz, $CDCl_3$) δ = (174.23), 174.00 (C═N), 170.91, 170.89, 170.67, 170.62, (170.38), 170.26, 170.22, (170.18), 169.60 (169.55) (C═O), 101.21, (101.09)/100.65 (C-1, C-1′), (80.87)/78.97 (CH), 76.12/(75.80) (C-4), (73.01)/72.81 (C-5), 72.58/(72.26) (C-3), 71.89 (C-2), (71.20)/70.85 (C-3′), 70.67 (C-5′), (69.05)/69.00 (C-2′), 66.50 (C-4′), 61.55/(61.33), 60.67/(60.63) (C-6, C-6′), (44.65)/43.80 (CH_2N), (41.23)/40.49 (CH_2NH), 36.35/(36.13) (α), 31.60 (ω-2), 29.28 (2), (29.20), 29.17, (29.07), 29.03 (2), 29.00 (bulk-CH_2), (25.33)/25.30 (β), 22.32 (ω-1), (20.50), 20.44 (2), 20.41, (20.37), 20.27 (3), 20.14 (Ac), 13.71 (ω). Elemental analysis for $C_{41}H_{64}N_2O_{18}$: C, 56.41; H, 7.39; N, 3.21, found: C, 57.54; H, 7.91; N, 3.74.

4.7.2. 2-Undecyl-5-β-lactosyl-1,4,5,6-tetrahydropyrimidine (15c)

Compound **14c** (0.5 g, 0.58 mmol) was deacetylated according to the procedure 4.1.4 to furnish (0.3 g, 93%) of compound **15c**. Mp 190 °C (dec). $[\alpha]_D^{25}$ +10.0 (*c* 0.15, CH_3OH). ^{1}H NMR (400 MHz, CD_3OD) δ = (4.47)/4.45, 4.36/(4.35) (2 × 2 d, 2H, H-1 & H-1′), 4.04–3.25 (m, 17H), 2.21 (t, 2H, α-CH_2), 1.61 (m_c, 2H, β-CH_2), 1.29 (m_c, 16H, bulk-CH_2), 0.90 (t, 3H, CH_3); $^3J_{1,2}$ = $^3J_{1',2'}$ = 8.0/7.5 Hz. ^{13}C NMR (100 MHz, CD_3OD) δ = 177.48 (C═N), 105.50, 105.35/(104.19) (C-1, C-1′), (80.74)/80.69, 80.27/(79.48), 77.32, 76.81, 76.50/(76.45), 75.04 (2)/74.86, 72.74, 70.48, 62.63, (62.03)/61.97 (C-6, C-6′), 45.49/(45.03) (CH_2N), (42.65)/41.60 (CH_2NH), 37.15/(37.02) (α), 33.01 (ω-2), 30.66 (2), 20.58, 30.39 (2), 30.28 (bulk-CH_2), (26.90)/26.87 (β), 23.62 (ω-1), 14.27 (ω).

4.8. Computer modeling

Initial modeling was performed in Chem3D. The structures were pre-optimized using MOPAC and then transferred into Gaussian 09. Structure optimization used a DFT approach based on the B3LYP theory and applying basis set 6-31G. The calculations took several days on an i7 cpu.

Acknowledgment

This work was supported by the University of Malaya under research grants PS382-2010B, RG026-09AFR and RP024-2012B.

Supplementary data

Supplementary data associated with this article can be found, in the online version, at http://dx.doi.org/10.1016/j.carres.2013.03.028.

References

1. Hymel, D.; Peterson, B. R. *Adv. Drug Deliv.* **2012**, *64*, 797–810.
2. Fuji, M.; Sata, Y.; Ito, H.; Masago, Y.; Omura, T. *J. Appl. Microbiol.* **2012**, *113*, 896–903.
3. Zhang, J.; Zhou, X. *Biosens. Bioelectron.* **2011**, *28*, 355–361.
4. Kulkami, A. A.; Fuller, C.; Korman, H.; Weiss, A. A.; Iyer, S. S. *Bioconjugate Chem.* **2010**, *21*, 1486–1493.
5. Okada, T.; Kimura, A.; Miura, H.; Nishiyama, T.; Mori, M.; Suzuki, J.; Ogiso, M.; Matsuoka, K.; Sato, T.; Hatanaka, K.; Minoura, H. *J. Carbohydr. Chem.* **2012**, *31*, 584–592.
6. Mannock, D. A.; Ruthven, R. N. A. H.; McElhaney, R. N. *Chem. Phys. Lipids* **1990**, *55*, 309–321.
7. Mannock, D. A.; Ruthven, R. N. A. H.; McElhaney, R. N.; Harper, P. E.; Turner, D. C.; Gruner, S. M. *Eur. Biophys. J.* **2001**, *30*, 537–554.
8. Sauvageeau, J.; Ryan, J.; Lagutin, K.; Sims, I. M.; Stocker, B.; Timmer, M. S. M. *Carbohydr. Res.* **2012**, *357*, 151–156.
9. Suzuki, T.; Harada, M.; Suzuki, Y.; Matsumoto, M. *J. Biochem.* **1984**, *95*, 1193–1200.
10. Minamikawa, H.; Murakami, T.; Hato, M. *Chem. Phys. Lipids* **1994**, *72*, 111–118.
11. Hashim, R.; Hashim, H. H. A.; Rodzi, N. Z. M.; Hussen, R. S. D.; Heidelberg, T. *Thin Solid Films* **2006**, *509*, 27–35.
12. Israelachvili, J. N.; Mitchell, D. J.; Ninham, B. W. *J. Chem. Soc., Faraday Trans. II* **1976**, *72*, 1525–1568.
13. Nguan, H. S.; Heidelberg, T.; Hashim, R.; Tiddy, G. J. T. *Liq. Cryst.* **2010**, *37*, 1205–1213.
14. Mikata, Y.; Shinohara, Y.; Yoneda, K.; Nakamura, Y.; Esaki, K.; Tanahashi, M.; Brudzinska, I.; Hirohara, S.; Yokoyama, M.; Mogami, K.; Tanase, T.; Kitayama, T.; Takashiba, K.; Nabeshima, K.; Takagi, R.; Takatani, M.; Okamoto, T.; Kinshita, I.; Doe, M.; Hamazawa, A.; Morita, M.; Nishida, F.; Sakakibara, T.; Orvig, C.; Shigenobu, Y. *J. Org. Chem.* **2001**, *66*, 3783–3789.
15. Vill, V.; Boecker, T.; Thiem, J.; Fischer, F. *Liq. Cryst.* **1989**, *6*, 349–356.
16. Gololobov, Y. G.; Zhmurova, I. N.; Kasuhin, L. F. *Tetrahedron* **1981**, *37*, 437–472.
17. Gololobov, Y. G.; Kasuhin, L. F. *Tetrahedron* **1992**, *48*, 1353–1406.
18. Zemplen, G.; Gerecs, A.; Hadacsy, I. *Ber. Dtsch. Chem. Ges.* **1936**, *69B*, 1827–1829.
19. Chen, Y.; Janczuk, A.; Chen, X.; Wang, J.; Kesebati, M.; Wang, P. G. *Carbohydr. Res.* **2002**, *337*, 1043–1046.
20. Gololobov, Y. G.; Gusar, N. I.; Chaus, M. P. *Tetrahedron* **1985**, *41*, 793–799.
21. Takeuchi, H.; Hagiwara, S.; Eguchi, S. *Tetrahedron* **1989**, *45*, 6375–6386.
22. Wu, L.; Burgess, K. *J. Am. Chem. Soc.* **2008**, *120*, 4089–4096.
23. Aspinall, S. L. *J. Am. Chem. Soc.* **1940**, *62*, 2160–2162.
24. Skinner, G. S.; Wunz, P. R. *J. Am. Chem. Soc.* **1951**, *73*, 3814–3815.
25. Brimblecombe, R. W.; Hunt, R. R.; Rickard, R. L.; Taylor, J. V. *Br. J. Pharmacol.* **1969**, *37*, 425–435.
26. Suhr, R.; Scheel, O.; Thiem, J. *J. Carbohydr. Chem.* **1998**, *17*, 937–968.
27. Dangate, M.; Franchini, L.; Ronchetti, F.; Arai, T.; Iida, A.; Tokuda, H.; Colombo, D. *Bioorg. Med. Chem.* **2009**, *17*, 5968–5973.
28. Ellens, H.; Siegel, D. P.; Alford, D.; Yeagle, P. L.; Boni, L.; Lis, L. J.; Quinn, J.; Bentz, J. *Biochemistry* **1989**, *28*, 3692–3703.
29. Chernomordik, L. V.; Zimmerberg, J. *Curr. Opin. Struct. Biol.* **1995**, *5*, 541–547.
30. Yu, Z. W.; Quinn, P. J. *Mol. Membr. Biol.* **1998**, *15*, 59–68.
31. Rendall, K.; Tiddy, G. J. T.; Tervathan, M. A. *J. Chem. Soc., Faraday Trans.* **1983**, *79*, 637–649.
32. Laughlin, R. G. *Adv. Colloid Interface Sci.* **1992**, *41*, 57–79.